Effect of Phospholipid Composition and Phase on Nanodisc Films at the Solid–Liquid Interface as Studied by Neutron Reflectivity

ARTICLE *in* LANGMUIR · FEBRUARY 2013

Impact Factor: 4.46 · DOI: 10.1021/la3024698 · Source: PubMed

5 AUTHORS, INCLUDING:

Robert Barker
University of Dundee
25 PUBLICATIONS **134** CITATIONS
SEE PROFILE

Kell Mortensen
University of Copenhagen
686 PUBLICATIONS **12,258** CITATIONS
SEE PROFILE

Robert Feidenhans'l
University of Copenhagen
136 PUBLICATIONS **2,936** CITATIONS
SEE PROFILE

Marité Cárdenas
Malmö University
54 PUBLICATIONS **793** CITATIONS
SEE PROFILE

Langmuir

Article

pubs.acs.org/Langmuir

Effect of Phospholipid Composition and Phase on Nanodisc Films at the Solid−Liquid Interface as Studied by Neutron Reflectivity

Maria Wadsäter,[†] Robert Barker,[‡] Kell Mortensen,[§] Robert Feidenhans'l,[§] and Marité Cárdenas*[,†]

[†]Nano-Science Center and Institute of Chemistry and [§]Nano-Science Center and Niels Bohr Institute, University of Copenhagen, Copenhagen, Denmark

[‡]Institut Laue Langevin, Grenoble, France

Supporting Information

ABSTRACT: Nanodiscs are disc-like self-assembled structures formed by phospholipids and amphipatic proteins. The proteins wrap like a belt around the hydrophobic part of the lipids, basically producing nanometer-sized patches of lipid bilayers. The bilayer in the nanodisc constitutes a native-like model of the cell membrane and can act as a nanometer-sized container for functional single membrane proteins. In this study, we present a general nanodisc-based system, intended for structural and functional studies of membrane proteins. In this method, the nanodiscs are aligned at a solid surface, providing the ability to determine the average structure of the film along an axis perpendicular to the interface as measured by neutron reflectivity. The nanodisc film was optimized in terms of nanodisc coverage, reduced film roughness, and stability for time-consuming studies. This was achieved by a systematic variation of the lipid phase, charge, and length of lipid tails. Herein, we show that, although all studied nanodiscs align with their lipid bilayer parallel to the interface, gel-phase DMPC nanodiscs form the most suitable film for future membrane protein studies since they yield a dense irreversibly adsorbed film with low roughness and high stability over time. This may be explained by the appropriate matching between the thickness of the hydrophobic lipid core of gel phase DMPC and the height of the belt protein. Moreover, once formed the gel-phase DMPC nanodiscs film can be heated up to melt the lipid bilayer, thus providing a more biologically friendly environment for membrane proteins.

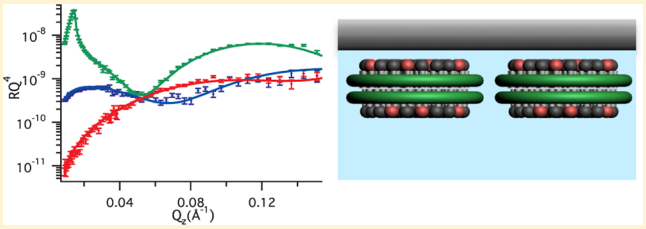

INTRODUCTION

Nanodiscs are self-assembled structures of proteins and lipids, which form small disc-like lipid bilayers. In these nanostructures, amphipathic helical proteins termed membrane scaffold proteins (MSPs) wrap like a belt around the hydrophobic part of a small patch of lipid bilayer,[1] enabling disc-like bilayers to be solubilized in an aqueous solution. The MSP was developed by genetic modification of the native apolipoprotein A-I that typically forms high-density lipoprotein particles in the blood. The apolipoprotein was optimized to form, upon lipid binding, monodisperse nanolipoprotein particles[1] in contrast to various apoliporoteins that tend to form various polydisperse particles.[2] By controlling the length of the MSP belt, the diameter of the disc is regulated giving nanometer-sized mimics of the cell membrane in which individual membrane proteins can be solubilized.[3−5] The monodispersity and particle size, in addition to the well-defined and consistent structure and stability over time, are examples of possible advantages of the nanodiscs compared to conventional membrane models as, for instance, vesicles or supported lipid bilayers (SLB).[5] The overall structure of the nanodisc, such as its overall dimensions and the orientation of the MSPs around a disc-like bilayer, was successfully characterized by small angle neutron scattering (SANS) and small angle x-ray scattering (SAXS).[6,7] The nanodiscs were proposed to possess an intrinsic elliptical shape[6] and tighter packing for phospholipids in nanodiscs than in liposomes.[8] SAXS data combined with differential scanning calorimetry (DSC) suggested that a fraction of the phospholipids in the nanodiscs (those along an approximately two-lipid thick rim around the MSP belt) do not participate in the cooperative lipid phase transition upon heating above the melting temperature of the phospholipids.[9] Additionally, time-resolved SAXS showed a 20-fold faster transfer of lipids between nanodiscs compared to liposomes.[8] Although the characterization of the empty nanodiscs resulted in new structural information, the inherent sensitivity of bulk scattering methods to the presence of minute amounts of aggregates in the solution places high demands on the quality of the sample in terms of monodispersity, and thus, these systems have been more challenging. The study of adsorbed nanostructures on surfaces accomplished by reflection-based techniques constitute an alternative approach to structural studies by SANS and SAXS of nanostructures in solution. For example, nanodiscs were shown to aligned in a well-ordered monolayer just below an oppositely charged surfactant layer at the air−water interface.[10]

Received: June 18, 2012
Revised: December 14, 2012
Published: February 1, 2013

   dx.doi.org/10.1021/la3024698 | *Langmuir* 2013, 29, 2871−2880

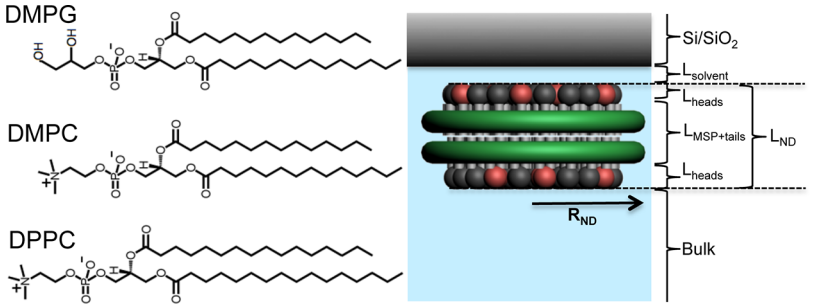

Figure 1. Left: Schematic drawing of the three phospholipids used in this study, DMPG, DMPC, and DPPC. Right: Either a 3-layer or a 1-layer model for the nanodisc was used in the fitting of the neutron reflectivity data.

The nanodisc film constitutes a platform for studies of the structure, folding, and function of membrane proteins. The nanodiscs not only minimize the presence of misfolded and dysfunctional proteins, but also could potentially allow the study of the effect of the physical properties of the lipid bilayer on the protein structure and function. Indeed, nanodiscs containing the membrane-anchored Cytochrome P450 Reductase (POR) were shown to align with the lipid bilayer parallel to the interface by neutron reflectivity.[11] Besides assessing the orientation of the nanodiscs and the overall conformation of the POR, this study allowed us to determine the changes in the conformational equilibrium upon addition of NADPH. This study also demonstrated that such surface-based systems are relatively insensitive to the presence of small amounts of aggregates and, more importantly, that the POR nanodiscs adsorbed with the water-soluble domain directed away from the solid surface.[11] The spontaneous proper orientation of the membrane protein containing nanodiscs, i.e., with the membrane protein being exclusively directed toward the bulk solution, makes the nanodisc-based system advantageous compared to SLB formed by vesicle fusion, as the direction of the membrane proteins in the lipid bilayer cannot be controlled in this case.[12]

Our study of POR-nanodiscs clearly demonstrated the applicability of this platform to study the structure and function of membrane proteins.[11] However, for nanodisc films to efficiently serve as a platform in reflectivity studies of membrane proteins in general, optimization of the nanodisc film was required. This optimization includes maximization of nanodisc coverage at the surface, as this coverage will determine the density of membrane proteins at the surface in membrane protein studies. Moreover, a well-ordered alignment of the nanodiscs with respect to the axis perpendicular to the interface and the stability of the film over time must be secured. Thus, the present study focuses on the structure of films of empty nanodiscs and addresses these issues. In particular, the effect of tail length and phase of the lipids on the structure of the nanodisc film were investigated using nanodiscs prepared from DPPC (C16) at 15 °C and DMPC (C14) at 15 and 30 °C. To create an environment similar to that of the native cell membrane that carries a net negative charge, nanodiscs made from mixtures of anionic and zwitterionic lipids (1:3 DMPG:DMPC) were also studied. The mass adsorption upon formation of the nanodisc film at the SiO_2 surface was monitored by quartz crystal microbalance with dissipation monitoring (QCM-D), while the detailed structure of the film was probed by neutron reflectivity (NR). The results suggest that gel-phase DMPC nanodiscs form the most dense and smooth films. The film can then be heated above the melting temperature of the DMPC (28 °C in nanodiscs[13]) to obtain lipid bilayer disks in the liquid crystalline-like phase, which may constitute a more native-like model of the environment in the cell membrane.

EXPERIMENTAL SECTION

The membrane scaffold protein used in this work was MSP1D1, which was expressed and purified according to Bayburt et al.[1] 1,2-Dimyristoyl-*sn*-glycero-3-phosphocholine (hDMPC), 1,2-dipalmitoyl-*sn*-glycerol-3-phosphocholine, 1,2-dimyristoyl-*sn*-glycero-3-phospho-(1′-rac-glycerol) (hDMPG), chain deuterated 1,2-dimyristoyl (d54)-*sn*-glycero-3-phosphocholine (dDMPC), and 1,2-dipalmitoyl (d54)-*sn*-glycero-3-phosphocholine (dDPPC) were all purchased from AVANTI and used as received; see Figure 1 for their chemical structures. Tris (pH 7.4) and NaCl (Sigma Aldrich) were dissolved in Milli-Q water or D_2O provided by the Institute Laue Langevin (ILL) prior to use. Nanodiscs were prepared as described elsewhere,[1,7] but in order to ensure lipid-filled nanodiscs, the nanodiscs were assembled from a 90:1 lipid:MSP mixture instead of 80:1 as previously used for nanodiscs made of DPPC.[7] All samples were filtered through 0.22 μm centrifugal filters (Millipore) followed by separation by size exclusion chromatography (Superdex 200 10/300 GL column, ÄKTA purifier system, GE Healthcare). The three most central 0.25 mL fractions of the nanodisc peak were pooled and used in further studies. The Si/SiO_2 substrate was pretreated by UV/ozone plasma cleaning (UV/Ozone ProCleaner, Bioforce Nanoscience, 10 min) or soaked in Piranha solution to obtain hydrophilic properties for QCM-D and NR surfaces, respectively. Nanodiscs in buffer (20 mM Tris, 100 mM NaCl, pH 7.4) solutions were injected to the NR and QCM-D cell. The temperature of the cell was set to 15 °C or to 30 °C for studies of nanodiscs with phospholipids in the gel and liquid crystalline phases, respectively. The anionic nanodiscs were adsorbed in either the presence or absence of 3 mM $MgCl_2$. The solution was left (15 min) in the cell to allow for adsorption of the nanodiscs to the SiO_2 surface and, upon steady-state conditions, extensive rinsing of the cell with buffer was performed.

Quartz Crystal Microbalance with Dissipation Monitoring (QCM-D). QCM is a nanogram-sensitive technique based on acoustic waves that measures the mass of an adsorbed film including the solution trapped in the layer. A quartz crystal is inserted between two gold electrodes, which due to its piezoelectric properties starts to oscillate when an AC voltage is applied.[14] The resonance frequency of the crystal decreases when mass adsorbs to it. This relation is linear for thin, rigid, evenly distributed films as described by the Sauerbrey equation.[15] However, in a liquid environment the viscosity of the liquid makes the linear relation inaccurate. The observed shift in frequency (Δf) will then be a result of both mass adsorption and viscoelastic energy dissipation. Additional information of the dissipative energy losses due to the viscoelastic properties of an adsorbed film in liquid can be obtained by the QCM-D technique, which monitors the dissipation (D) directly by measuring the amplitude decay of the oscillations after the applied voltage is turned off.[16] In this study, a Q-Sense E4 system was used.

dx.doi.org/10.1021/la3024698 | *Langmuir* 2013, 29, 2871−2880

Neutron Reflectivity (NR). Neutrons are scattered by the nucleus of an atom. The ability to scatter neutrons depends not only on the atomic nucleus, but also on the isotopes of the same element. This property allows designing and optimizing contrast between different components in a sample by varying the isotope composition. The ability to scatter neutrons of a particular component is quantified by a scattering length density (ρ), which can be calculated as $\rho = \sum_i (b_i/V)$, where b_i is the coherent scattering length of each nuclei i in a given volume, V. In a NR experiment, the intensity of specular (mirror-like) reflected neutrons (R) is measured as a function of the scattering vector ($\mathbf{Q}_z$) perpendicular to the interface ($\mathbf{Q}_z = ((4\pi/\lambda)\sin\theta)$, where θ is the angle of reflection and λ is the neutron wavelength). The reflectivity is related to the scattering length density of the material on the surface via an inverse Fourier transformation.[17] The experiment provides the averaged composition (ρ) and structure of the interface material along an axis perpendicular to the interface. The advantage of using neutrons to study biological systems arises particularly from the different scattering lengths of the isotopes hydrogen and deuterium,[18] which allows for contrast variation by deuterium substitution for hydrogen since this typically has negligible chemical and biological effects. The reflectivity profiles obtained in this study were analyzed by fitting a simulated reflectivity curve of a model structure of the system to the experimental data using the software *Motofit*.[19] This software uses the Abeles optical matrix method to calculate the reflectivity of thin layers, and it also enables simultaneous fitting of data sets of different isotopic compositions by using a genetic fitting approach.[20] The neutron reflection experiments were performed at the FIGARO beamline[21] at Institute Laue-Langevin, France.

Two different types of silicon crystals, with roughness of 6 Å (rough) or 3 Å (smooth) were used in this study. The clean Si/SiO_2 substrate was precharacterized in order to fit the thickness and roughness of the SiO_2 layer as well as the fraction of solvent in the SiO_2 layer, which is present in the cavities arising from the irregularities of the SiO_2 interface. These parameters were kept constant in the subsequent fitting process. The nanodisc film was modeled as a single layer (L_{ND}), for which the thickness (t_{ND}), coverage (ϕ_{ND}), and roughness in the inner and outer interface ($r_{solvent/ND}$ and $r_{ND/bulk}$) were fitted. A thin solvent layer ($L_{solvent}$) between the nanodiscs and the solid substrate was necessary to properly fit the data, which also has been observed for supported lipid bilayers.[22] This solvent layer thickness is typically of the same order of magnitude as the substrate roughness and represents the water trapped within the roughness of the SiO_2 surface, which is too small to incorporate lipid head groups. The hDMPC nanodisc film adsorbed to smooth substrates with a roughness of 3 Å was also modeled using three different layers; lipid heads (L_{heads}), the central body composed of the hydrophobic lipid tails and the two MSP1D1s ($L_{MSP+tails}$) and again lipid heads (L_{heads}). The thicknesses ($t_{solvent}$, t_{head}, $t_{MSP+tail}$, and t_{head}) and coverage (ϕ_{head}, $\phi_{MSP+tail}$, and ϕ_{head}) of the layers and the interfacial roughness between the layers ($r_{solvent/head}$, $r_{head/MSP+tail}$, $r_{MSP+tail/head}$, and $r_{head/bulk}$) were fitted. The models used to represent the nanodisc by one and three layers are shown schematically in Figure 1. In either case, it was assumed that each nanodisc contained 180 phospholipids, as measured by phosphor analysis (for a description of this analysis see Supporting Information, Methods). The nanodiscs were modeled by using constant volumes (Table S1 in the Supporting Information) of the lipids and MSP1D1s. The lipids were modeled as cylinders and the two MSP1D1 proteins were modeled as a uniform belt with a thickness equal to that of the lipid tails from the two leaflets. As listed in the Supporting Information Table S1, the volume of the MPS1D1 estimated by SAXS for DLPC nanodiscs at 20 °C[6] was used in all models. The volume of the lipid tails (V_{tails}) is expected to increase upon melting. On the contrary, the volume of the headgroup (V_{heads}) in fully hydrated lipid bilayers is typically expected to be constant, since the lipid heads are completely immersed in water in both the gel and fluid phases.[23] Indeed, the number of water molecules per lipid head in POPC nanodiscs observed from SAXS data is similar to that reported for the headgroup in liposomes.[6] Thus, a constant volume of the headgroup of the nanodisc seems as a reasonable assumption. Nevertheless, a 20% expansion of the lipid heads upon melting gives only a 4% larger nanodisc volume, which lies within the error of the measurement. All calculated scattering length densities used in this work are listed in the Supporting Information Table S1. The scattering length density of the nanodiscs in the 1-layer model was calculated from the average weight of the lipid tail, lipid heads, and protein according to $\rho_{ND} = \rho_{MSP}\chi_{MSP} + \rho_{tails}\chi_{tails} + \rho_{heads}\chi_{heads}$, where ρ_{MSP}, ρ_{tails}, and ρ_{heads} and χ_{MSP}, χ_{tails}, and χ_{heads} are the scattering length density and volume fraction of the MSP1D1 protein belts, the lipid tails, and the lipid heads, respectively. In case of the 1:3 DMPG:DMPC nanodiscs, the difference in ρ between the two lipid heads were taken into account by using a weighted average instead, using the respective volume fractions and scattering length densities of each lipid. In the case of the 3-layer model, the area per lipid head (A_{head}) and the area per lipid tails (A_{tails}) were kept equal according to $A_{head} = (V_{head}/t_{head}) = A_{tails} = (V_{tails}/t_{tails})$ in order to ensure a physically realistic nanodisc model. The scattering length density of the nanodiscs in L_{heads} was calculated by including the solvent that is present on top of the MSP1D1 belt, in the disc with radius $R_{ND} = (A_{ND}/\pi)^{1/2}$ (Figure 1), where $A_{ND} = ((180V_{tails} + 2V_{MSP})/t_{MSP+tails})$ is the area of the nanodisc in $L_{MSP+tails}$. Thus, in layer L_{heads} the coverage of the disc with radius R_{ND} was fitted, which included solvent. A constraint $\phi_{head} = \phi_{MSP+tail}$ ensured that A_{heads} and A_{tails} was kept equal.

The parameters for the best models were found using a global genetic fitting while monitoring the χ^2 values of the fit simultaneously on all three sets of data. The uncertainty of the model fit (Table 2) was estimated by determining the maximum accepted deviation of each parameter separately allowing a 5% variation from the global minimum χ^2 value. "Synthetic data" were generated while each parameter was varied. Moreover, possible cross-correlations between parameters such as thickness and coverage between the same layer and among different layers was used by 2D plots of χ^2 coverage and taking the parameter value extremes at 5% variation from the minimum χ^2 value. This was performed by systematic comparison of the "synthetic" and experimental data in all available contrasts.[22]

RESULTS

Nanodisc Film Formation. The adsorption of nanodiscs prepared from phosphatidylcholine lipids with different lengths of hydrocarbon chains C14 (DMPC) or C16 (DPPC) and negatively charged nanodiscs containing a mixture of DMPC and a phosphatidylglycerol (DMPG) (1:3 DMPG:DMPC) were monitored in situ by QCM-D. The adsorptions were studied at 15 and 30 °C under continuous flow (0.1 mL/min), and the results upon steady-state conditions and after extensive rinsing with buffer solution are summarized in Table 1. This table includes QCM-D values for Δf, D, and Sauerbrey mass for

Table 1. Shift in Frequency, Dissipation, and Sauerbrey Mass of Adsorbed Nanodisc Made of DMPC, DPPC, and 1:3 DMPG:DMPC ($\pm$3 mM $MgCl_2$) as Measured by QCM-D[a]

nanodisc	concentration (nM)	Δf (Hz)	D (10^{-6})	Sauerbrey mass (ng/cm^2)
DMPC (15 °C)	600	27.5 ± 1	0.2 ± 0.1	487 ± 18
DMPC (15 °C)	300	27 ± 1	0.2 ± 0.1	478 ± 18
DMPC (15 °C)	60	25.5 ± 1	0.1 ± 0.1	451 ± 18
DMPC (15 °C)	30	24.5 ± 1	0.2 ± 0.1	434 ± 18
DMPC (30 °C)	300	23.5 ± 1	0.2 ± 0.1	416 ± 18
DPPC	300	30 ± 1	0.3 ± 0.1	531 ± 18
1:3 DMPG:DMPC	300	25 ± 1	0.2 ± 0.1	442 ± 18
1:3 DMPG:DMPC + 3 mM $MgCl_2$	300	24.5 ± 1	0.2 ± 0.1	434 ± 18

[a]The values are the steady state values after extensive flushing with buffer solution.

dx.doi.org/10.1021/la3024698 | *Langmuir* 2013, 29, 2871−2880

Table 2. Model Fits to Neutron Reflectivity Data of Nanodiscs Prepared from Different Phospholipids for Discs Adsorbed from a Bulk Concentration of 600 nM

	T (°C)	$r_{surface}$ (Å)[a]	$t_{solvent}$ (Å)	t_{ND} (Å)	ϕ_{ND} (v/v%)	$r_{solvent/ND}$ (Å)	$r_{ND/bulk}$ (Å)
hDMPC	15	3	6 ± 1	39 ± 1	64 ± 2	3 ± 2	3 ± 2
hDMPC	15	6	6 ± 1	40 ± 1	37 ± 2	6 ± 2	6 ± 2
dDMPC	15	6	5 ± 1	39 ± 2	56 ± 2	5 ± 2	4 ± 2
dDMPC	30[b]	6	5 ± 1	35 ± 2	61 ± 3	9 ± 3	6 ± 2
dDMPC	30	6	–	38 ± 5	30 ± 5	14 ± 4	14 ± 4
dDPPC	15	6	5 ± 1	43 ± 1	52 ± 2	9 ± 2	10 ± 2
1:3 DMPG:DMPC +3 mM $MgCl_2$	15	3	8 ± 1	39 ± 2	54 ± 3	3 ± 2	3 ± 2
1:3 DMPG:DMPC	15	3	7 ± 1	39 ± 2	47 ± 3	3 ± 3	4 ± 2

[a]The roughness of the substrates was found prior nanodisc adsorption and fixed to these values during analysis of the nanodisc film. [b]The nanodiscs were adsorbed at 15 °C and thereafter heated to 30 °C.

the adsorption various nanodiscs at different concentrations. At 15 °C, DMPC, DMPG, and DPPC are all expected to exist in the gel phase.[24] At 30 °C, however, DMPC nanodiscs are expected to be in the liquid crystalline phase.

Table 1 shows that the dissipation remained low (below 0.3 × 10^{-6} dissipation units) during the adsorption of all the different nanodiscs regardless of lipid phase and presence of 3 mM $MgCl_2$, indicating that rigid films are formed in all cases. For rigid films, the Sauerbrey equation[15] can be used to estimate the adsorbed mass that includes the solvent within the layer. Due to the uncertainties in the estimate of the amount of water that couples to the film, in addition to the small difference in density of hDMPC nanodiscs (1.14 g/cm^3) and the aqueous solution, the dry absolute coverage of nanodiscs at the surface cannot be accurately determined from the adsorbed mass measured via QCM-D. Nevertheless, the Sauerbrey mass can be used for qualitative comparisons among the different nanodisc adsorptions. For instance, we note that the obtained wet masses for DMPC nanodiscs are fairly constant above 300 mM and at 15 °C. Slightly higher mass was obtained for DPPC. Moreover, similar increase in dissipation was measured upon formation of dDPPC and dDMPC nanodiscs films (Table 1), the larger frequency shift for DPPC nanodiscs is probably due to the larger weight of the DPPC nanodiscs (~9% higher weight of the film is expected for DPPC films as compared to DMPC films). Thus, from the QCM-D data we expect similar surface area coverage for DMPC vs DPPC nanodiscs.

For DMPG containing nanodiscs at 15 °C, the total change in frequency (and wet mass) for the negatively charged nanodiscs was lower than for DMPC nanodiscs. Interestingly, the measured f and D shifts at saturation conditions were independent of the presence of $MgCl_2$ in the subphase (Table 1).

For all concentrations used, the gel-phase DMPC nanodiscs quickly formed a saturated film. As expected, the adsorption kinetics increased the higher the nanodisc concentration (saturation is reached within about 1.5 min for 600 and 300 nM, 7 min for 60 nM and 10 min for 30 nM; see Supporting Information Figure SI 1). Although the differences in adsorbed mass between the different concentrations are not significant, repeated adsorptions did show a trend of slightly larger frequency shifts for increasing nanodisc concentration. A maximum of 12% difference in adsorbed mass was measured among the concentrations studied.

The stability of the nanodisc film over time and its resistance to mechanic removal due to liquid flow is demonstrated by the small change in frequency (less than 1 Hz in 30 min) measured during constant flow with buffer, which is only slightly higher than the drift of the Q-Sense E4 system (1 Hz in 60 min).[25] The stability of the DMPG containing nanodiscs, on the other hand, against extensive rinsing with Mg^{2+} free buffer was poorer than for pure PC nanodiscs, since rinsing with buffer led to a slow desorption process (about 9% within the first 15 min).

In contrast to the QCM-D results (Table 1), the neutron reflectivity curve changed significantly as the nanodisc concentration was raised from 60 to 600 nM (see Figure SI 2). For 60 nM, very little nanodisc adsorption occurred. For 600 and 1500 nM, the reflectivity profiles were similar demonstrating that saturation was achieved at 600 nM (Figure SI 2). Note, however, that the bulk concentration necessary to saturate the film could very well be below 600 nM, since no intermediate concentration was tested in between 60 nM and 600 nM due to restricted beam time availability. Both reflectivity profiles for 600 and 1500 nM are very much alike, and thus the formation of nanodisc film is reproducible once film saturation conditions are reached. Moreover, these adsorptions were performed using sample arising from different nanodiscs preparations, which confirm that the reflectivity profiles presented in this work did not depend on differences in sample preparation. Indeed, the size exclusion chromatogram for different nanodisc preparations were highly reproducible as shown for DMPC and 1:3 DMPG:DMPC nanodiscs in Figure SI 3. In this respect, using the apolipoprotein ApoE422k and DMPC Blanchette et al.[26] demonstrated large polydispersity within the nanodisc retention peak upon size exclusion of a single nanodisc preparation. However, SAXS studies showed that monodispersed nanodiscs can indeed be prepared with high reproducibility using the MSP1D1 belt protein and under controlled assembly conditions (e.g., lipid/protein stoichiometry and temperature).[6,27] Moreover, Blanchette et al.[26] suggested collecting small aliquots from the nanodisc retention peak after size exclusion to effectively reduce the polydispersity of the nanolipoprotein particles prepared from ApoE422k and DMPC. Indeed, for the samples used in our study, only ~30% of the total peak volume at the very center of the nanodisc retention peak was collected as shown for DMPC and 1:3 DMPG:DMPC nanodiscs in Figure SI 3. Instead, the different nanodisc concentration required to reach the maximum nanodisc adsorption as measured by NR and QCM-D could be explained by differences in flow—and thus mass transfer to the interface—between the neutron and QCM-D liquid cells, as well as the difference in the substrate roughness, which is below 1 nm in our neutron reflection setup while it is 3−4 nm for QCM-D sensors (as determined using AFM). All neutron reflectivity experiments were hereafter performed using 600 nM nanodiscs. Finally, extensive rinsing with buffer solution did not

dx.doi.org/10.1021/la3024698 | Langmuir 2013, 29, 2871−2880

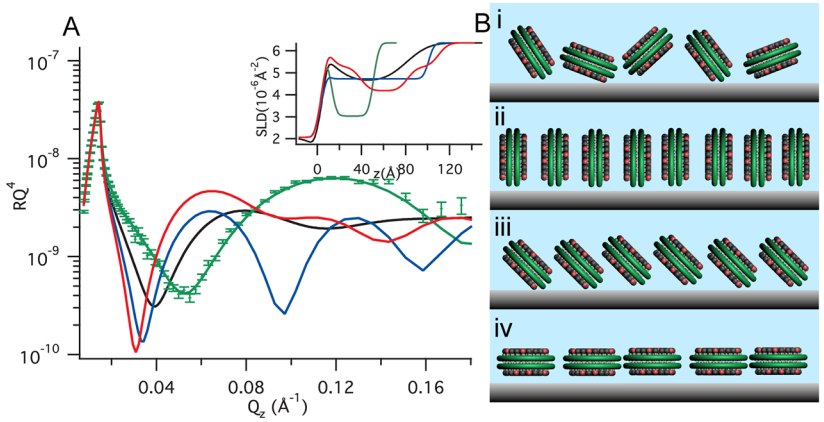

Figure 2. Reflectivity data for hDMPC nanodisc film and the simulated reflectivities in D_2O (A) for different orientations of nanodiscs at the solid−liquid interface, as schematized in (B). A model of nanodisc film formed by (i) random adsorption (black line in A), (ii) having the lipid bilayer perpendicular to the interface (blue line in A), or (iii) tilted by 45° with respect to the surface (red line in A) does not properly fit the experimental data (green symbols). Only the model of nanodiscs adsorbed with the lipid bilayer parallel to the surface (green line in A) can represent the reflectivity data. The inset in A shows the fitted scattering length density profiles perpendicular to the interface for the various models schematized in B.

significantly affect the reflectivity profile even upon 8 h after film formation (Figure SI 4), demonstrating the irreversible nature of the adsorption process and the stability of the film.

Overall Alignment of Nanodisc Films. Simulated reflectivity curves of various possible orientations of nanodiscs at the interface were compared to the experimental reflectivity data (Figure 2A,B) for DMPC nanodiscs at 15 °C adsorbed at 600 nM in D_2O. The simulated curve of a model of nanodiscs adsorbed with random orientation did not fit the experimental data (Figure 2B,i). In this case, the random nanodisc orientations were accounted by fitting a model of a single layer with higher roughness and thickness than that for a nanodisc monolayer in which the lipid bilayer is parallel to the underlying surface (the diameter of the nanodiscs is ∼10 nm, while their height is only 4 nm). This means that the film must possess some structural order. Strong interactions between the MSP and the solid substrate and/or between lipid heads in different nanodiscs could result in a film of nanodiscs adsorbed with their lipid bilayer perpendicular or tilted (45°) with respect to the interface as shown in Figure 2B, ii and iii, respectively. However, none of the corresponding simulated reflectivity curves in Figure 2A fit the data as well as that of the model of nanodisc adsorbed with their lipid bilayer parallel to the surface (Figure 2B, iv).

Detailed Structure of hDMPC Nanodisc Films in the Gel Phase. Figure 3 gives neutron reflectivity profiles for the nanodisc film formed upon exposure of 600 nM hDMPC nanodisc solution to a silicon crystal at 15 °C in D_2O buffer after flushing the liquid cell with pure D_2O, pure H_2O, and a H_2O/D_2O−mixture (cmSi) with a H_2O/D_2O ratio equal to 2.07 that ensures contrast matching conditions to the Si-support (Figure 3).

A model of a (39 ± 1)-Å-thick nanodisc layer could be fitted to all three contrasts simultaneously. The obtained thickness corresponds very well to that of DMPC lipid bilayers below the melting temperature (40 Å).[28] Note that the errors in the best model allow for maximally 10% of the nanodiscs in the film to be oriented perpendicular to the interface. The best fit indicates that the nanodisc film is separated from the solid support by a thin (5 Å) solvent layer and the film covers (64 ± 2)% of the surface.

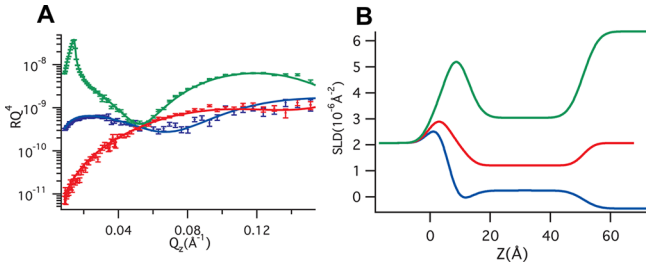

Figure 3. (A) Neutron reflectivity data (markers) of hDMPC nanodiscs (15 °C) in D_2O (green), H_2O (blue), and cmSi (red). The adsorption was performed at nanodisc concentration of 600 nM. The solid lines are the simulated reflectivity curves of the model that gave the best fit. (B) Scattering length density profiles perpendicular to the interface corresponding to the model fits.

The roughness of the hDMPC nanodisc film (3 ± 2 Å) is the same as that of the solid substrate (3 Å), which is as low as that of capillary waves on the water surface.[29] The low roughness of the adsorbed layer could, in principle, allow for extraction of more structural details of the film. However, the use of a model containing three different layers (L_{head}, $L_{MSP+tails}$, and again L_{heads}) yields equally good fits as those using a single layer (Figure SI 5 and Table SI 2). Thus, our measurements (Figure 3) did not allow differentiation between the tail and the headgroup region in the nanodisc layer, which is typically necessary for SLB.[22]

Effect of Substrate Roughness. hDMPC nanodiscs were also adsorbed to a substrate with higher roughness (6 Å) under similar conditions as those used in Figure 3, and the measured reflectivity curves in D_2O, H_2O, and cmSi are shown in Figure 4. In this fit, we obtained similar thicknesses of the nanodisc film and the solvent layer to that of the smooth surface. However, the film roughness had to be increased to 6 ± 2 Å to properly fit the data. It is unlikely that the increased roughness is a result of particle polydispersity or variance among different nanodisc preparations, since the reflectivities measured for two different preparations generated undistinguishable curves (Figure SI 2). Instead, the result indicates that the roughness of the substrate propagates into the nanodisc film. The higher roughness also seemed to impair the interactions between the

dx.doi.org/10.1021/la3024698 | Langmuir 2013, 29, 2871−2880

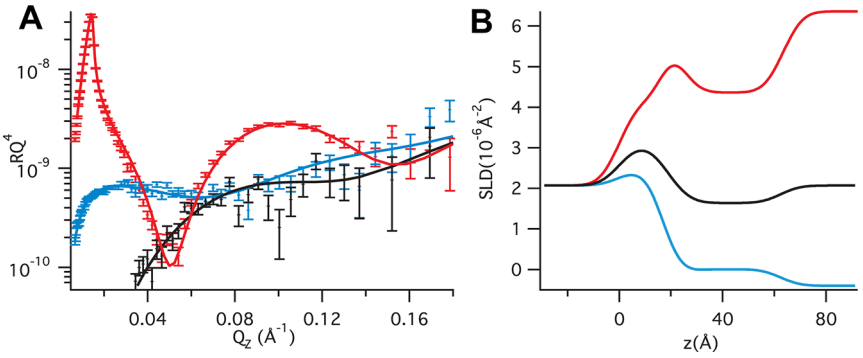

Figure 4. (A) Neutron reflectivity curves of the hDMPC nanodiscs film on a rough (6 Å) SiO_2 substrate in D_2O (red symbols), H_2O (blue symbols), and cmSi (black symbols). The reflectivity in cmSi was only measured in the large angle. The solid curves are the fits to single-layer mode. The fitted scattering length density profiles perpendicular to the interface are shown in (B).

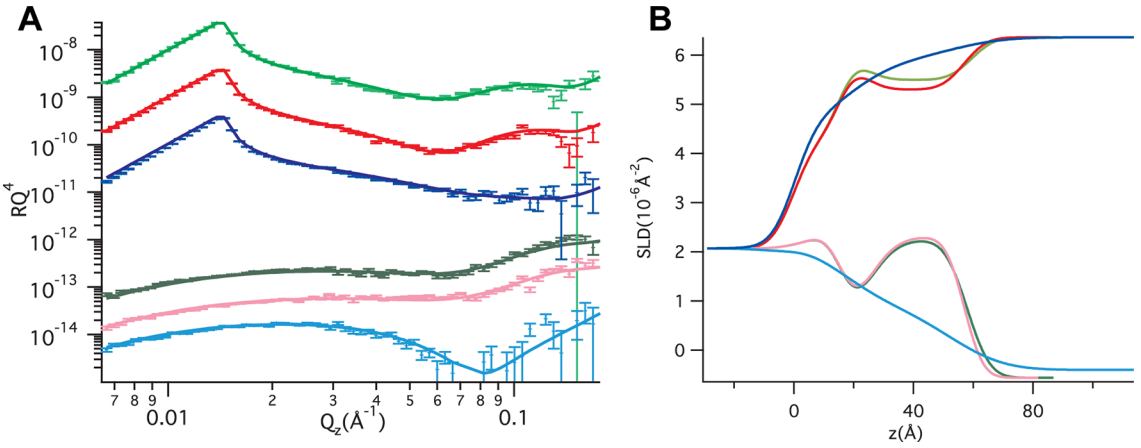

Figure 5. (A) Neutron reflectivity of the dDMPC nanodisc film adsorbed from a bulk solution of 600 nM in either the gel phase at 15 °C (D_2O, light green and H_2O, dark green) or thereafter heated to 30 °C to attain the liquid crystalline phase (D_2O, red and H_2O, pink). The figure also includes a nanodisc film formed at 30 °C in the liquid crystalline phase (D_2O, blue and H_2O, light blue). The data have been shifted vertically for better display. (B) Scattering length density profiles perpendicular to the interface for the models given in (A).

lipid heads and the surface, as the coverage of the different nanodiscs was found to be lower (37−56 v/v%) at the rougher surface. Reduced adsorption of surfactants at rougher substrates was previously observed at silica surfaces.[30] This illustrates the importance of using smooth substrates in, for instance, detailed studies of membrane proteins reconstituted in nanodiscs, as roughness limits the resolution in a reflectivity experiment also due to impaired surface coverage.

Effect of Deuteration of the Lipid Tail. Gel-phase dDMPC nanodiscs were adsorbed to the rougher surface under similar conditions than for hDMPC, and the resulting reflectivity curves are shown in Figure 5. The dDMPC film showed similar thickness and roughness of the nanodisc and solvent layer as for hDMPC nanodiscs (Table 2), as expected. However, the reflectivity curve of deuterated samples in D_2O is very sensitive to the presence of small amounts of hydrogenated molecules at the surface. The use of nanodiscs containing deuterated lipids shows that the film besides nanodiscs also contains low amounts of lipid-free MSP1D1, as the fit for the nanodisc model in the absence of lipid-free MSP1D1 gives different dDMPC nanodisc coverage for the different isotropic bulk contrasts measured (D_2O, H_2O, and cmSi). In order to maintain a constant dDMPC nanodisc coverage (56 v/v%) for all three contrasts, 4 v/v% lipid-free MSP1D1 is required in the adsorbed nanodisc film. The hydrogenated nanodisc film most likely also contains similar amounts of lipid-free MSP1D1, but the contrast of the system makes the reflectivity insensitive to the presence of such small fractions of free protein: The inclusion of 4 v/v% lipid-free MSP1D1 at the surface in the model of the hDMPC nanodisc film only changes the hDMPC coverage with less than 2.5 v/v% units compared to that in the absence of lipid-free MSP1D1, and is thus within the error of the fit for hDMPC nanodiscs.

Interestingly, considerable differences in coverage were observed for hDMPC and dDMPC nanodisc films on silica surfaces (37% vs 56%, respectively). The reason behind this phenomenon is not yet completely understood, although deuteration effects on coverage were reported earlier for nanodisc films at the air−water interface[10] and surfactant layers at the solid−liquid interface.[30]

Effect of Lipid Phase. Figure 5 includes reflectivity profiles for the same dDMPC nanodisc films after heating above the melting temperature of the lipids in the nanodiscs[9,10] (30 °C), and also reflectivity data for dDMPC nanodiscs adsorbed in the liquid crystalline phase (30 °C). Upon heating of the nanodiscs that were preadsorbed in gel phase, only small changes in the reflectivity curves are measured. The main minimum in the reflectivity profiles move to larger Q_z corresponding to thinning of the film. For the liquid crystalline dDMPC nanodiscs, the best fits (Table 2) propose a lipid bilayer thickness of 35 ± 2 Å and a slight increase in surface coverage (61 ± 3%). This result is consistent with the lateral expansion of phospholipids upon

dx.doi.org/10.1021/la3024698 | Langmuir 2013, 29, 2871−2880

melting, which previously was observed in nanodiscs[6,9] and demonstrates the extensibility of the MSP1D1. The obtained thicknesses of the DMPC nanodiscs in both the gel and the liquid crystalline phase are 10−12 Å lower than those previously observed by SAXS in nanodiscs.[9] However, the thickness of fluid-phase DLPC (C12) and POPC (C16−C18) nanodiscs was found to be 33.8 and 42.7 Å in another SAXS study,[6] in agreement with our result once we take into account the difference in hydrocarbon tail length. The number of nanodiscs per unit area at the surface in the gel (15 °C) and liquid crystalline phase (30 °C) was calculated by using the fitted coverage and thickness of the nanodisc film and the volumes of the lipids and MSP1D1 given in Table SI 1. The calculation gives the same number of nanodiscs per unit area in both phases, which suggests that no desorption is accompanied by the heating of the film and also validates the chosen model.

The reflectivity curves of dDMPC nanodisc adsorbed in the liquid crystalline phase are considerably different from the ones absorbed in the gel phase (Figure 5). The thickness of the nanodiscs is, as for the nanodiscs heated after adsorption, thinner, but the nanodisc coverage (30 v/v%) is substantially lower (Table 2). This is consistent with the smaller shift in frequency accompanied by the adsorption of DMPC nanodiscs in the liquid crystalline phase compared to those in gel phase as measured by QCM-D (Table 1).

Finally, the model that generated the best fits for fluid-phase nanodiscs did not require the presence of an intermediate solvent layer, while the roughness of the nanodisc film was significantly higher (14 Å) than for gel-phase nanodiscs (6 Å). The lack of a water layer in this case could be related to the higher interfacial roughness of nanodiscs in the fluid phase and the fact that the lipids are in the fluid phase and could potentially better couple to the surface. Since this is the only sample measured above the lipid T_m, we cannot uniquely conclude if this property is indeed related to the physical state of the lipids. Finally, the neutron reflection experiment cannot discern whether the origins of the higher nanodisc roughness arise from either a less well-defined nanodisc structure or a less ordered alignment of the nanodisc film in the liquid crystalline phase.

Effect of Lipid Tail Length. The reflectivity curves of gel-phase dDPPC nanodiscs adsorbed to a rough surface at 15 °C are shown in Figure 6 at a bulk nanodisc concentration of 600 nN. The structure of the film resembles that of the d/hDMPC nanodisc film (Table 2) in terms of the presence of a thin solvent layer and similar nanodisc coverage. A very slight change in thickness was measured via NR for the dDPPC (43 ± 1 Å) and the dDMPC (39 ± 2 Å) nanodisc films (Table 2). This is a surprisingly small difference given that DPPC has two additional carbon groups on each hydrocarbon chain as compared to DMPC and that the thickness of gel-phase lipid bilayers has been measured to be 52 Å for DPPC[31] and 40 Å for DMPC.[28]

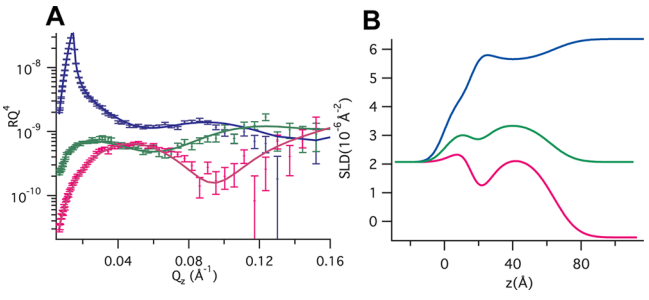

Figure 6. (A) Neutron reflectivity curves of the gel-phase dDPPC nanodisc (15 °C) adsorbed from a concentration of 600 nM in D_2O (blue), H_2O (green), and cmSi (pink). (B) Scattering length density profiles perpendicular to the interface found from the model fits.

Interestingly, the roughness of the DPPC nanodisc film is higher (9 Å) than for DMPC nanodisc films (6 Å). Again, the origin of the roughness cannot be addressed by neutron reflectivity, but in general, it could arise from either a less well-defined nanodisc structure or a less ordered alignment of the nanodiscs in the liquid crystalline phase at the surface. The higher roughness of DPPC nanodiscs as compared to DMPC nanodiscs in combination with the almost constant thickness for DMPC and DPPC nanodiscs do, however, suggest that the lipids in the nanodiscs adopt slightly different conformation than in unconstrained lipid bilayers.

Effect of Lipid Charge. The native cell membrane possesses a slight negative charge. It is thus, in this context, desirable to create stable, smooth, and dense films of nanodiscs prepared from negatively charged lipids. Nanodiscs made 1:3 DMPG:DMPC were adsorbed in the same buffer (20 mM Tris, 100 mM NaCl, pH 7.4) as the nanodiscs made of zwitterionic lipids. The reflectivity curve of the anionic nanodisc (in 93 v/v % D_2O) adsorbed to the smooth SiO_2 substrate and in the presence of 3 mM $MgCl_2$ is shown in Figure 7. The reflectivities measured in D_2O and H_2O after extensive rinsing with $MgCl_2$ free buffer are also shown in the figure. As compared to DMPC nanodiscs, neither the thickness nor the roughness of the nanodisc film is affected by the presence of the fraction of DMPG (Table 2). The negatively charged nanodiscs are, however, more distant from the substrate (8 ± 1 Å) than neutral nanodiscs. In agreement with QCM-D data (Table 1), the 1:3 hDMPG:hDMPC nanodiscs form a slightly less dense film (54 v/v% in the presence of 3 mM $MgCl_2$) than the neutral DMPC nanodiscs (64 v/v%) at the smooth substrate. Furthermore, after extensive rinsing (approximately 5 exchanges of cell volume) of the liquid cell, and consequent removal of $MgCl_2$, about 13% of the nanodiscs at the surface desorb, yielding a final stable coverage of 47 v/v%. This desorption is indeed comparable to the 9% measured via QCM-D (Table 1) under continuous rinsing with Mg-free buffer. The introduction of 25% charged phospholipids to the nanodisc is thus not changing the structure of the nanodisc, but repulsion between the nanodiscs and the negative SiO_2 surface results in weaker interactions and thus less dense and stable films.

DISCUSSION

In this study, the adsorption and structure of nanodisc films on silicon substrates was measured by QCM-D and neutron reflectivity with the aim to create a dense, smooth, and well-ordered nanodisc film. Such films could serve as a platform system for structural and functional studies of membrane proteins as demonstrated recently.[11] Neutron reflectivity shows that DMPC, DPPC, and 1:3 DMPG:DMPC nanodiscs all align with their lipid bilayer parallel to the interface (Figure 2−7). However, the theoretical 2D packing of circular or elliptical objects (91%) is not reached under any of the conditions used, as the surface area covered by the nanodiscs, ϕ_{ND}, only reaches a maximum of ∼60% (Table 2). For gel-phase PC nanodiscs, the high reproducibility in nanodisc coverage indicates a physical/chemical origin of this value (Table 2). The MSP1D1 is, like other helical apolipoproteins,[32,33] expected to carry a net

dx.doi.org/10.1021/la3024698 | Langmuir 2013, 29, 2871−2880

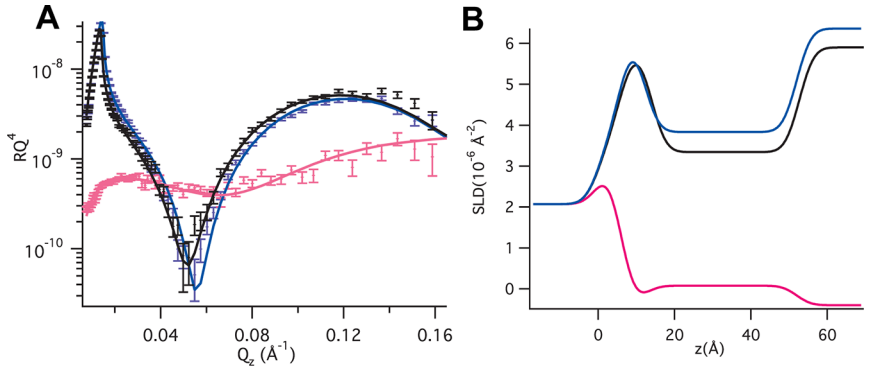

Figure 7. (A) Neutron reflectivity curves of gel-phase 1:3 hDMPG:hDMPC nanodiscs (15 °C) adsorbed from a solution containing 600 nM nanodiscs and $MgCl_2$ in 93 v/v% D_2O (black), after rinsing off the Mg^{2+} in D_2O (blue) and H_2O (pink). (B) Scattering length density profiles perpendicular to the interface found from the model fits.

charge. Lateral electrostatic repulsion between MSP1D1s in neighboring nanodiscs could thus prevent closer packing of nanodiscs. However, if repulsion between adjacent nanodiscs controlled the nanodisc coverage alone, a surface coverage of approximately 80% should be achievable as calculated including one Debye length (9 Å) at the conditions used. Thus, other factors than just electrostatics are expected to interfere with the nanodisc packing. The flanking polyhistidine tag[6] (His-tag) linked to the N-terminal region of the MSP1D1 could create an additional steric hindrance for closer packing. Assuming that the His-tag undertakes the conformation of a noncompressible Gaussian random coil with a radius of gyration of 12.7 Å[6] and that one His-tag bridges two neighboring nanodiscs, a maximum nanodisc coverage of ~60% is obtained. Moreover, besides being irreversibly adsorbed (Table 1, Figure SI 4), the nanodiscs may also be kinetically trapped and immobilized (incapable to diffuse and reorient within the plane) upon adsorption. Such adsorption and fixation of nanodiscs at random positions on a SiO_2 surface will give a scattered pattern in which the internanodisc separation is larger than in a hexagonal packing but still too small to accommodate additional nanodiscs. A lower coverage than the theoretical maximum will thus be obtained.

On the other hand, the adsorbed film of nanodiscs with gel-phase DMPC is denser than that formed by adsorption of nanodiscs with their lipids in the liquid crystalline phase as measured by both neutron reflection (Figure 5, Table 2) and QCM-D (Table 1). Moreover, the liquid crystalline DMPC nanodiscs are forming a rougher layer with respect to the axis perpendicular to the surface (Table 1). SAXS studies of nanodiscs showed that the disc-like bilayer structure is also retained in the liquid crystalline phase.[6,9] Thus, our NR results suggest that nanodiscs, adsorbed in the fluid phase, have a lower affinity for the surface. The chemophysical details behind this observation are not yet well-understood. One possibility is that the changes in the tilt of the phosphorus−nitrogen dipole of the phosphatidylcholine head groups in the fluid and gel phase (0−3° and 30° with respect to the membrane plane,[34,35] respectively) could impair the interaction between the nanodiscs and the SiO_2 surface and thus the film density.

The thickness of the nanodisc lipid bilayer is less dependent on lipid tail length and phase than in supported lipid bilayers (Table 2). Moreover, both the gel-phase DPPC (Figure 6) and the liquid crystalline DMPC nanodisc films (Figure 5) are rougher than the gel-phase DMPC (Figure 5) nanodiscs. These observations suggest that the MSP belt controls the thickness of the lipid bilayer in the nanodiscs. A hydrophobic mismatch between the MSP belt and the hydrophobic lipid tails[6,9] may affect the lipid packing at the rim of the MSP belt so as to match the hydrophobic thickness of the belt.[6] From the expected thickness of the two α-helices of the MSP belt,[6] gel-phase DMPC should give a more accurate hydrophobic match. The difference in lipid bilayer thickness between the rim and the core of disc is thus expected to be more drastic for nanodiscs composed of DPPC than for DMPC giving slightly convex DPPC nanodiscs. In a reflectivity experiment, a film made of such nanodiscs will appear to have increased interfacial roughness. The same reasoning could then be applied to the higher roughness measured for dDMPC nanodiscs in the liquid crystalline phase. Given that the thickness of free supported DMPC bilayers in gel and liquid crystalline phase is 41.9 and 35.1 Å, respectively,[36] melting of the lipids in the nanodiscs will give a thinning of the nanodisc core only, resulting in a slightly concave structure of fluid-phase DMPC nanodiscs. Besides the higher film roughness, such a hydrophobic match will give an average lipid bilayer thickness in the nanodiscs that is less dependent on the lipid phase (39 ± 2 Å versus 35 ± 2 Å for gel and fluid dDMPC nanodiscs, respectively) or tail length (43 ± 1 Å versus 39 ± 2 Å for dDPPC and dDMPC, respectively) than in SLB, since the lipid bilayer is then strongly controlled by the height of the MSP1D1 belt.

Additionally, our measurements (Figure 3) did not allow differentiation between the tail and the headgroup region in the nanodisc layer, which is typically necessary for SLB.[22] The presence of MSP in the tail layer results in a smaller difference in scattering length density (~1.4×10^{-6} Å^{-2}) between the nanodisc core (MSP + lipid tails) and the lipid head groups than between the corresponding layers in supported hDMPC bilayers (~2.3×10^{-6} Å^{-2}). Moreover, irregular wrapping of the MSP belt around the bilayer or interdigitation of the belt protein and the lipid head groups will smear out the layers into a single one.

To further mimic the native environment of the cell membrane, a film of nanodiscs made from mixtures of anionic and zwitterionic lipids (1:3 DMPG:DMPC) were studied (Figure 7). Negatively charged nanodiscs gave films similar to the neutral DMPC nanodiscs in terms of thickness and roughness (Table 2). However, the film was more distant from the underlying substrate, the nanodisc coverage is slightly lower, and the film less stable as compared to DMPC nanodiscs. The lower coverage and poorer stability against increasing buffer of DMPG containing nanodiscs was

dx.doi.org/10.1021/la3024698 | Langmuir 2013, 29, 2871−2880

corroborated by QCM-D experiments (Table 1). At the ionic conditions used, both the SiO_2 surface and the nanodiscs are expected to be negatively charged. The surface charge density of silica at pH 7.4 is ~0.25 OH^-/nm,[2,37] while the estimated surface charge for the zwitterionic DMPC and DPPC nanodiscs is ~0.1 e^-/nm^2 and for the negatively charged 1:3 DMPG:DMPC nanodiscs is ~0.4 e^-/nm^2 (hereby we assume that the compositions of the nanodiscs are the same as in the nominal preparation[38] and that the net charge of the MSP1D1 is −6.9). Although four times stronger repulsion is expected between the anionic DMPG nanodiscs and the SiO_2 surface, the presence of divalent ions was not required for the anionic nanodisc film to be formed as is typically the case for SLB formed by vesicle fusion.[39,40] This suggests that other interactions besides electrostatics are responsible for the nanodisc film formation (protein−surface or histag−surface for instance).

Finally, this study demonstrates the importance of the quality of the substrate in terms of roughness, as substrate roughness reflected not only on the film roughness but also on the nanodisc surface coverage (Figures 3 and 4). In summary, the best nanodiscs for studies of membrane proteins in nanodiscs at a solid SiO_2 surface are gel-phase DMPC nanodiscs, as these form relatively dense films with low roughness. Moreover, this system allows for studies of membrane proteins in the liquid crystalline phase (a more biologically relevant environment), since the film can be heated to the fluid phase after adsorption without leading to nanodiscs desorption (Figure 5).

■ ASSOCIATED CONTENT

Supporting Information

Additional figures and tables. This material is available free of charge via the Internet at http://pubs.acs.org.

■ AUTHOR INFORMATION

Corresponding Author

*Telephone: + 45 35 32 04 69. E-mail: cardenas@nano.ku.dk.

Notes

The authors declare no competing financial interest.

■ ACKNOWLEDGMENTS

The authors acknowledge financial support from "Center for Synthetic Biology" at Copenhagen University funded by the UNIK research initiative of the Danish Ministry of Science, Technology and Innovation and DANSCATT center funded by the Danish government for financial support. We thank the Institute Laue Langevin (ILL) in France for the DOE under neutron reflectivity experiment (Ex N°: 9-13-321). We acknowledge Tomas Laursen and Peter Naur for kindly providing us with the MSP1D1 and Jens B. Simonsen for illustrative drawings. We thank Per Hedegård for discussions.

■ REFERENCES

(1) Bayburt, T. H.; Grinkova, Y. V.; Sligar, S. G. Self-assembly of discoidal phospholipid bilayer nanoparticles with membrane scaffold proteins. *Nano Lett.* **2002**, *2* (8), 853−856.

(2) Chromy, B. A.; Arroyo, E.; Blanchette, C. D.; Bench, G.; Benner, H.; Cappuccio, J. A.; Coleman, M. A.; Henderson, P. T.; Hinz, A. K.; Kuhn, E. A.; Pesavento, J. B.; Segelke, B. W.; Sulchek, T. A.; Tarasow, T.; Walsworth, V. L.; Hoeprich, P. D. Different apolipoproteins impact nanolipoprotein particle formation. *J. Am. Chem. Soc.* **2007**, *129*, 14348−14354.

(3) Borch, J.; Hamann, T. The nanodisc: a novel tool for membrane protein studies. *Biol. Chem.* **2009**, *390*, 805−814.

(4) Ritchie, T. K.; Grinkova, Y. V.; Bayburt, T. H.; Denisov, I. G.; Zolnerciks, J. K.; Atkins, W. M.; Sligar, S. G., Reconstitution of Membrane Proteins in Phospholipid Bilayer Nanodiscs. In *Enzymology*; Academic Press, 2009; Vol. *464*.

(5) Nath, A.; Atkins, W. M.; Sligar, S. G. Applications of Phospholipid Bilayer Nanodiscs in the Study of Membranes and membrane protein. *Biochemistry* **2007**, *46*, 2059−2069.

(6) Skar-Gislinge, N.; Simonsen, J. B.; Mortensen, K.; Feidenhans'l, R.; Sligar, S. G.; Moller, B. L.; Bjornholm, T.; Arleth, L. Elliptical Structure of Phospholipid Bilayer Nanodiscs Encapsulated by Scaffold Proteins: Casting the Roles of the Lipids and the Protein. *J. Am. Chem. Soc.* **2010**, *132* (39), 13713−13722.

(7) Denisov, I. G.; Grinkova, Y. V.; Lazarides, A. A.; Sligar, S. G. Directed Self-Assembly of Monodisperse Phospholipid Bilayer Nanodiscs with Controlled Size. *J. Am. Chem. Soc.* **2004**, *126*, 3477−3487.

(8) Nakano, M.; Fukuda, M.; Kudo, T.; Miyazaki, M.; Wada, Y.; Matsuzaki, N.; Endo, H.; Handa, T. Static and Dynamic Properties of Phospholipid Bilayer Nanodiscs. *J. Am. Chem. Soc.* **2009**, *131* (23), 8308−8312.

(9) Denisov, I. G.; McLean, M. A.; Shaw, A. W.; Grinkova, Y. V.; Sligar, S. G. Thermotropic phase transition in soluble nanoscale lipid bilayers. *J. Phys. Chem. B* **2005**, *109* (32), 15580−15588.

(10) Wadsäter, M.; Simonsen, J. B.; Lauridsen, T.; Grytli Tveten, E.; Naur, P.; Bjørnholm, T.; Wacklin, H.; Mortensen, K.; Arleth, L.; Feidenhans'l, R.; Cardenas, M. Aligning Nanodiscs at the Air Water Interface, a Neutron Reflectivity Study. *Langmuir* **2011**, *27*, 15065−15073.

(11) Wadsäter, M.; Laursen, T.; Singha, A.; Hatzakis, N. S.; Barker, R.; Mortensen, K.; Feidenhans'l, R.; Lindberg Møller, B.; Cárdenas, M. Monitoring Shifts in the Conformation Equilibrium of the Membrane Protein Cytochrome P450 Reductase (POR) in Nanodiscs. *J. Biol. Chem.* **2012**, *297*, 34596−34603.

(12) Kiessling, V.; Domanska, M. K.; Murray, D.; Wan, C.; Tamm, L. K., Supported Lipid Bilayers: Development and Applications in Chemical Biology. *Wiley Encyclopedia of Chemical Biology*; John Wiley & Sons, Inc., 2008.

(13) Shaw, A. Phospholipid phase transitions in homogeneous nanometer scale bilayer discs. *Febs Lett.* **2004**, *556* (1−3), 260−264.

(14) Marx, K. A. Quartz Crystal Microbalance- A Useful Tool for Studying Thin Polymer Films and Complex Biomolecular Systems at the Solution-Surface Interface. *Biomacromolecules* **2003**, *4*, 1099−1120.

(15) Sauerbrey, G. Verwendung von Schwingquarzen zur Wägung Dünner Schichten und zur Mikrowägung. *Z. Physik* **1959**, *155*, 206−222.

(16) Dixon, M. C. Quartz Crystal Microbalance with Dissipation Monitoring- Enabling Real-Time Characterization of Biological Materials and Their Interactions. *Journal of Biomolecular Technique* **2008**, *19*, 151−158.

(17) Majkrzak, C. F.; Satija, S. K.; Berk, N. F.; Borchers, J. A.; Dura, J. A.; Ivkov, R.; O'Donovan, K. *Neutron News* **2001**, 25−29.

(18) Jacrot, B. The study of biological structures by neutron scattering from solution. *Rep. Prog. Phys.* **1976**, *39*, 911−953.

(19) Nelson, A. Co-refinement of multiple-contrast neutron/X-ray reflectivity data using MOTOFIT. *J. Appl. Crystallogr.* **2006**, *39* (2), 273−276.

(20) Abeles, F. *Ann. Phys.* **1948**, *3*, 504−520.

(21) Campbell, R. A.; Wacklin, H. P.; Sutton, I.; Cubitt, R.; Fragneto, G. FIGARO: The new horizontal neutron reflectometer at the ILL. *The European Physical Journal Plus* **2011**, *126*, 11.

(22) Vacklin, H. P.; Tiberg, F.; Fragneto, G.; Thomas, R. K. Composition of Supported Model Membranes Determined by Neutron Reflection. *Langmuir* **2005**, *21*, 2827−2837.

(23) Nagel, J. F. Stucture of lipid bilayers. *Biochim. Biophys. Acta* **2000**, *1469*, 159−195.

(24) Heimburg, T. *Thermal Biophysics of Membranes*; WILEY-VCH Verlag GmbH, Weinheim, 2007.

(25) http://q-sense.com/ (August 20th, 2012).

(26) Blanchette, C. D.; Segelke, B. W.; Fischer, N.; Corzett, M. H.; Kuhn, E. A.; Cappuccio, J. A.; Benner, W. H.; Coleman, M. A.; Chromy, B. A.; Bench, G.; Hoeprich, P. D.; Sulchek, T. A. Characterization and purification of polydisperse reconstituted lipoproteins and nanolipoprotein particles. *Int. J. Mol. Sci.* **2009**, *10* (7), 2958−71.
(27) Denisov, I. G.; Grinkova, Y. V.; Lazarides, A. A.; Sligar, S. G. Directed self-assembly of monodisperse phospholipid bilayer nanodiscs with controlled size. *J. Am. Chem. Soc.* **2004**, *126* (11), 3477−3487.
(28) Tristram-Nagle, S.; Liu, Y.; Legleiter, J.; Nagle, J. F. Structure of Gel Phase DMPC Determined by X-Ray Diffraction. *Biophys. J.* **2002**, *83*, 3324−3335.
(29) Braslau, A.; Deutsch, M.; Pershan, P. S.; Weiss, A. H.; Als-Nielsen, J.; Bohr, J. Surface Roughness of Water Measured by X-Ray Reflectivity. *Phys. Rev. Lett.* **1985**, *54* (2), 114−117.
(30) Fragneto, G. Neutron Reflection from Hexadecyltrimethylammonium Bromide Adsorbed on Smooth and Rough Silicon Surfaces. *Langmuir* **1996**, *12*, 6036−6043.
(31) Åkesson, A.; Lind, T.; Ehrlich, N.; Stamou, D.; Wacklin, H.; C ardenas, M. Composition and structure of mixed phospholipid supported bilayers formed by POPC and DPPC. *Soft Matter* **2012**, *8*, 5658−5665.
(32) Segrest, J. P.; Jackson, R. L.; Morriset, J. D. A molecular theory of Lipid-protein interactionc in the plasma membrane. *FEBS Lett.* **1974**, *38*, 247−253.
(33) MacRaild, C. A.; Howlett, G. J.; Gooley, P. R. The Structure and Interactions of Human Apolipoprotein C-II in Dodecyl Phosphocholine. *Biochemistry* **2004**, *43*, 8084−8093.
(34) Hauser, H.; Pascher, I.; Pearson, R. H.; Sundell, S. Prefered conformation and molecular packing of phosphatidylethanolamine and phosphatidylcholine. *Biochim. Biophys. Acta* **1981**, *650*, 21−51.
(35) Pink, D. A.; Belaya, M.; Levadny, V.; Quinn, B. A Model of Polar Group Statics in Lipid Bilayers and Monolayers. *Langmuir* **1997**, *13*, 1701−1711.
(36) Hughes, A. V.; Roser, S. J.; Gerstenberg, M.; Goldar, A.; Stidder, B.; Feidenhans'l, R.; Bradshaw, J. Phase Behavior of DMPC Free Supported Bilayers Studied by Neutron Reflectivity. *Langmuir* **2002**, *18*, 8161−8171.
(37) Bolt, G. H. Determination of the Charge Density of Silica Sols. *J. Phys. Chem.* **1957**, *61*, 1166.
(38) Wadsäter, M.; Selma, M.; Simonsen, J.; Mortensen, K.; Cárdenas, M. The Effect of Using Binary Mixtures of Zwitterionic and Charged Lipids on the Nanodisc Formation and Stability; *Soft Matter* **2013**, *9*, 2329−2337.
(39) Cho, N. J.; Frank, C. W.; Kasemo, B.; Hook, F. Quartz crystal microbalance with dissipation monitoring of supported lipid bilayers on various substrates. *Nat. Protoc.* **2010**, *5* (6), 1096−106.
(40) Åkesson, A.; Lind, T. K.; Barker, R.; Hughes, A.; Cárdenas, M. Unraveling Dendrimer Translocation across Cell Membrane Mimics. *Langmuir* **2012**, *28*, 13025.